## 5.3
## Routes for the Preparation of Isolated Oxide Nanoparticles

5.3.1
Hydrolysis

Traditionally, a number of oxide materials have been prepared from aqueous solution using hydrolytic methods. Many of these preparation techniques lend themselves to the preparation of nanoparticles. The term hydrolysis is used in a number of contexts, in most of which it involves breaking up of the water molecule [34]. It is useful to imagine that the hydrolysis of a hydrated trivalent metal ion into an oxide takes place in the following manner:

$$2M^{3+}(H_2O)_6 \rightarrow M_2O_3\downarrow + 6H^+ + 9H_2O$$
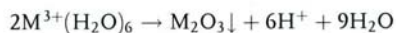
Such a scheme indicates that the water molecule is decomposed in the process and, in addition, that the formation of an oxide usually requires basic conditions. However, in the preparation of oxides of amphoteric species such as Al(III) or Ga(III), acid hydrolysis could be employed. For example:

$$2[Ga(OH)_4]^- \rightarrow Ga_2O_3\downarrow + 3H_2O + 2(OH)^-$$
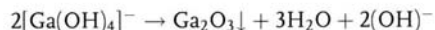
An important aspect of such hydrolysis is that not all ions are amenable to it. The alkali, alkaline earth and rare-earth ions, for example, are too stable in solution, and too ionic for hydrolysis to take place. In fact, the hydration reaction is the one that would be favored. For La^{3+} for example, the equilibrium:

$$La_2O_3\downarrow + 6H^+ + 9H_2O \leftrightarrow 2La^{3+}(H_2O)_6$$
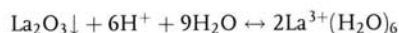
can be shifted completely to the left only at temperatures as high as 1000 K.

Despite these limitations, hydrolytic routes have been the mainstay of many preparations of nanoparticulate oxide materials, particularly of the first row transition metals. It is of interest to note that much of the reported literature on hydrolytic routes concerns aqueous systems and it would not be incorrect to say that much needs to be done on the use of solvents other than water, particularly aprotic solvents, where hydrolysis may be more effective. The use of electrochemistry to assist in hydrolysis is a technique that has found much use in the preparation of transition metal oxide films [35], but it's use in the preparation of oxide nanoparticles is not widespread.

Magnetic oxide (typically ferrite spinels or γ-Fe$_2$O$_3$) nanoparticles, when dispersed at high concentrations in water or oil, form ferrofluids [36]. Particle sizes in these materials are usually in the 5–15 nm range – small enough that neither magnetic nor gravitational fields should cause their precipitation. The many uses of ferrofluids in magnetic seals, bearings, dampers etc. [36] have resulted in an extensive body of literature on the preparation and properties of dispersions of

magnetic oxide nanoparticles. Many of the preparative routes involve hydrolysis. In many cases, the preparation simply involves raising the pH of a solution of metal ions, taken in the correct proportion, by addition of base. Sorenson, Klabunde and coworkers [37], have made detailed magnetic and Mössbauer studies of $MnFe_2O_4$ nanoparticles prepared by precipitation at high pH followed by digestion. Cabuil and coworkers [38] have shown in the case of the preparation of $CoFe_2O_4$ and γ-Fe_2O_3 particles that changing the temperature and the nature of the base allows particles of different sizes to be prepared. In addition, they have suggested methods of dispersing the particles in water, through controlling Coulomb repulsion between the particles. The particles can be dispersed in oils by modifying their surfaces with long chain surfactants. Cabuil et al. [39] have also shown that size-selection of particles is possible though control of a combination of surface charge and ionic strength of the dispersing medium. Morales et al. [40] have made a careful study of γ-Fe_2O_3 nanoparticles, with sizes ranging from 3 to 14 nm, prepared by hydrolytic means (and also by laser pyrolysis of $Fe(CO)_5$ in solution). They show that to account for the magnetic properties of the particles, it is necessary to use a model wherein the moments on the surface of the particle are canted.

The use of polar solvents other than water to perform hydrolysis is an exciting prospect. Ammar et al. [41] have demonstrated that glycols (specifically 1,2-propanediol) can be used as a solvent under reflux to hydrolyze a mixture of Co(II) and Fe(III) salts to obtain equiaxed particles of $CoFe_2O_4$ with an average diameter of 5.5 nm. A combination of Mössbauer spectroscopy, X-ray absorption near-edge structure (XANES) and magnetic measurements suggested that the particles were well-ordered both in terms of being crystalline and having all Co in the divalent state. Rajamathi et al. have been able to capitalize on the unusual properties of glycols – that they are sufficiently polar that they can dissolve metal salts and that they can support hydrolysis and yet they can dissolve long chain surfactants such as amines – in the preparation of n-octylamine-capped 5 nm γ-Fe_2O_3 nanoparticles [42]. The particles [Figure 5.2] can be dissolved in toluene when a little excess amine is added to the solvent. The particles can be precipitated through addition of a polar solvent such as 2-propanol, and then redissolved in toluene/n-octylamine. Diethylene glycol has also been used as a solvent by Carunto et al. [43] to prepare a number of transition metal ferrites capped by long chain carboxylic acids.

Pileni [44] has reviewed the extensive work from her group on the use of reverse micelles as nanoscale reaction chambers within which nanoparticles can be prepared. In a system of water and surfactant dispersed in oil, under suitable conditions, the water forms spherical droplets of radius R_W given by:

$$R_w = \frac{3V_{aq}[H_2O]}{\sigma[S]}$$

where square brackets indicate concentration, S refers to surfactant, σ is the area per head group of the surfactant molecule and V_{aq} is the volume of a water molecule. By controlling the water and surfactant concentration, the diameter of the water droplet can therefore be controlled. If a nanoparticle is nucleated within the
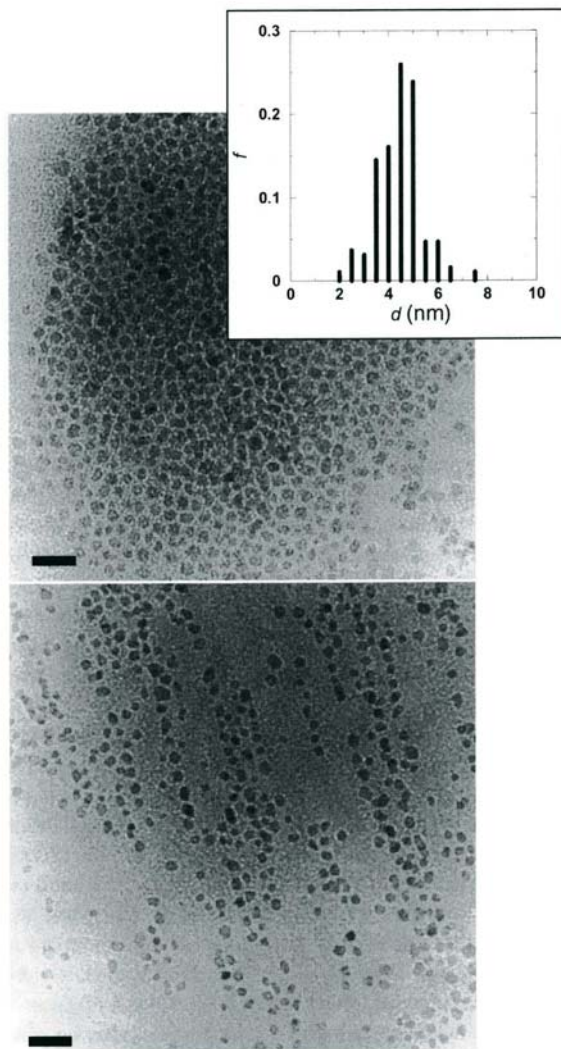
Fig. 5.2. Transmission electron micrographs of maghemite γ-Fe$_2$O$_3$ nanoparticles prepared by hydrolysis of Fe(III) salts in refluxing propylene glycol in the presence of amine capping agents. The nanoparticles are soluble in toluene solutions of n-octylamine and, as a result, display a tendency for superlattice self-assembly when concentrated (top) and to form aligned arrays in the direction of the earth's magnetic field when dilute (bottom). The bars are 20 nm. Reproduced from [42] with permission from the Royal Society of Chemistry.

water sphere, its growth is limited by the size constraint of the water droplet. Pillai and Shah [45] have utilized this route to prepare high-coercivity $CoFe_2O_4$ nanoparticles by mixing two water-in-oil microemulsions, one containing metal ions and the other containing base. These authors calcine the particles, so the resulting material is nanophase, rather than nanoparticulate. $MnFe_2O_4$ [46] and $CoCrFeO_4$ [47] have been prepared using such reverse-micelle routes by Zhang et al., and characterized by using a combination of magnetization studies and powder neutron diffraction.

Pileni has also pioneered the use of the surfactant-as-reactant approach in the preparation of nanoparticles. For example, in the preparation of $CoFe_2O_4$ nanoparticles with sizes between 2 and 5 nm, instead of preparing inverse-micellar dispersions of the Co and Fe salts, Moumen and Pileni [48] prepared the dodecylsulfonate (DS) analogs $Fe(DS)_2$ and $Co(DS)_2$. These were made to form micellar solutions, to raise the pH, aqueous methylamine solution was added. Stirring for 2 h resulted in a magnetic precipitate. Due to the low yield of Fe(II) to Fe(III) oxidation under these conditions, an excess of $Fe(DS)_2$ is required.

With an increase in concentration of the reactants, there is an increase in particle size. Zinc-doped cobalt ferrite nanoparticles [49] and zinc ferrite [50] have also been prepared using these methods. The 10 nm ferrite nanocrystal ferrofluids prepared using the $Fe(DS)_2$ route form deposits with different morphologies when evaporated on oriented graphite substrates [51]. The morphology can be strongly influenced by applying a magnetic field during the evaporation process. Thus magnetic properties of deposits prepared in the presence and absence of a field are quite different.

Hydrolysis can be assisted by using irradiation of the reacting bath with ultrasound. In these sonochemical preparations, acoustic cavitation results in the production of concentrated spots of extremely high temperatures. These "hot spots" accelerate the rate of metal ion hydrolysis. Gedanken and coworkers [52] have prepared ZnO, CuO, Co_3O_4 and Fe_3O_4 particles by subjecting solutions of the acetates to ultrasound irradiation using a high-intensity horn. Particle morphologies could be altered by using mixtures of water and dimethyl formamide instead of pure water as the solvent. Magnetite nanorods have been prepared by these authors [53] by ultrasonically irradiation of Fe(II) acetate in water in the presence of β-cyclodextrin. The authors suggest that cyclodextrin molecules are acting as size-stabilizing agents.

5.3.2
Oxidation

Oxides, unlike the other chalcogenides (sulfides, selenides, tellurides), are not associated with an oxide ion source. In other words, while the formation of a sulfide such as ZnS can be written:

$$Zn^{2+} (aq.) + S^{2-} (aq.) \rightarrow ZnS\downarrow$$
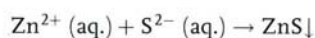
where the source of the sulfide ion in solution could be Na_2S or thiourea or the like, it is not possible to frame a similar reaction scheme for oxides. On the other hand, it is possible to directly oxidize a metal source in solution. A popular route to this is to use zero-valent carbonyls, for example $Fe(CO)_5$. Decomposing these carbonyls in solvents results in very finely divided metal particles that are easily susceptible to oxidation. In fact, exposing them to an atmosphere of air is usually sufficient to convert the particles to oxides.

Bentzon et al. [11] have prepared iron oxide nanoparticles by decomposing $Fe(CO)_5$ in decalin in the presence of oleic acid as the stabilizing ligand. Aging the ferrofluid so formed in air for several weeks results in a mixture of hematite and spinel phases. The fascinating aspect of this work is that it is among the first reports of nanocrystal superlattice formations, and is still only one of few reports on highly coherent oxide nanocrystal superlattices. More recently, Hyeon et al. have prepared monodisperse γ-Fe_2O_3 nanoparticles in the size range 4–16 nm by decomposing $Fe(CO)_5$ complexes in octyl ether at 300 °C in the presence of oleic acid. Oxidation of bcc-Fe to γ-Fe_2O_3 was achieved by the addition of the organic oxidant $(CH_2)_2NO$. The resulting capped oxide nanoparticles can easily be redispersed in organic solvents such as hexane or toluene. Particle sizes are altered by varying the ratio of Fe to the capping agent (oleic or lauric acids). The remarkable feature of this preparation is that the as-prepared particles are sufficiently monodisperse that they form nanocrystal superlattices without the need for a size-selection process.

Wagner and coworkers have prepared yttrium oxide [55] and europium-doped yttrium oxide nanoparticles [56] by first reducing rare-earth salts in solution using alkalides (strong reducing agents that are complexes of crown ethers with alkali metals, and where the anion is a complexed electron) and then oxidizing the rare-earth metal nanoparticle so formed, in aerated water. The white powders were then annealed in air. Some more examples of oxide nanoparticles prepared through direct oxidation will be discussed in the solvothermal methods section.

5.3.3
Thermolysis

If one starts with a precursor complex wherein the ligands bind to metal ions through oxygen, it could be possible to envisage a decomposition reaction that would leave behind the metal oxide.

For a trivalent ion, such reactions could be generalized as:

$$[R-O]_3-M^{3+} \rightarrow M_2O_3 + \text{leaving groups}$$
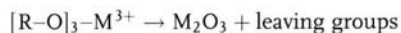
Suitable design of the R group (stable leaving groups) would ensure that the reaction proceeds in a facile manner. It should then be possible to carry out such reactions in a suitable high temperature solvent under solvothermal conditions, possibly in the presence of a suitable capping agent.

Rockenberger, Scher and Alivisatos [57] have described the use of cupferron complexes as precursors to prepare transition metal oxide nanoparticles. Cupferron (*N*-phenyl, *N*-nitroso hydroxylamine) forms bidentate, univalent complexes with a number of different transition metals ions. These complexes easily decompose to give the oxide. The authors demonstrated the preparation of γ-Fe_2O_3, Cu_2O and Mn_3O_4 nanoparticles prepared by injecting octylamine solutions of the corresponding cupferron precursors into refluxing trioctylamine. Size is controlled by controlling the temperature of the reaction. The particles so prepared form stable solutions in solvents such as toluene, from which they can be reprecipitated by the addition of methanol. This work is quite seminal in its generality, and particularly in the manner it which it suggests the search for suitable precursors for the preparation of oxide nanoparticles. Most importantly, it suggests thermolysis as an alternative to hydrolysis which, as pointed out earlier, is simply not viable for a number of metal oxides.

An important contribution to the surface chemistry of metal oxide nanoparticles has been made by Rotello and coworkers [58] who have prepared γ-Fe_2O_3 nanoparticles by the cupferron decomposition method, and compared the relative efficacies of different long chain surfactants as capping agents. The most stabilizing capping agent (as monitored by ease of redissolution and stability in solution) was obtained by using a two-tailed surfactant (with 12-carbon tails) with the polar part comprising a 1,3-diol.

The thermolysis of Fe(III) hydroxide caprylates in boiling tetralin under argon flow gives γ-Fe_2O_4 nanoparticles [59]. The surfaces of the nanoparticles could be modified by exchanging the capping caprylate groups with betaine, among other species [60]. Betaine-capped γ-Fe_2O_3 nanoparticles are reported to have high solubility in water. Using a combination of hydrolysis and oxidation, O'Brien, Brus and Murray [61] have shown that the treatment of a complex alkoxide containing Ba^{2+} and Ti^{4+}, $BaTi(O_2CC_7H_{15})[OCH(CH_3)_2]_5$, an agent for the MOCVD growth of $BaTiO_3$, can be decomposed in diphenyl ether at 140 °C, in the presence of oleic acid as a capping agent, to give nanocrystalline, cubic $BaTiO_3$ [Figure 5.3]. After cooling to 100 °C, 30% H_2O_2 is added, and crystallization is induced over a 48 h period. Changing the ratio of capping agent to water, and the amount of peroxide added, permits the size of the particles to be varied. This is perhaps the only report of soluble perovskite oxide nanoparticles and, once again, is a route of great generality and interest. The authors also report using such routes to prepare $PbTiO_3$ and TiO_2 nanoparticles.

5.3.4
Metathesis

In a metathetic reaction, two compounds AB and CD, exchange species to give two new compounds AC and BD. Such routes have been explored in the preparation of nanoparticles. Arnal et al. [62] have reported two non-hydrolytic routes to sol–gel metal oxides, particularly of titanium. The first route involves the reaction of a metal halide with a metal alkoxide:
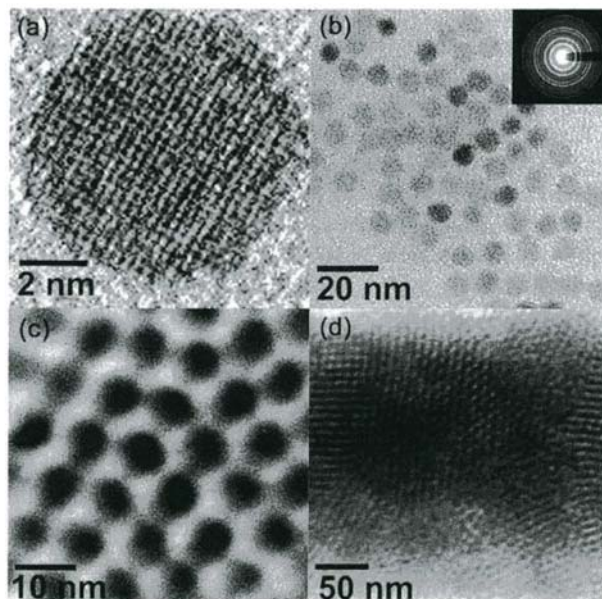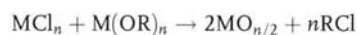
Fig. 5.3. Transmission electron micrographs of 8 nm BaTiO$_3$ nanoparticles prepared by the hydrolysis/oxidation of a Ba–Ti alkoxide precursor. Reproduced from [61] with permission from the American Chemical Society.

$$MCl_n + M(OR)_n \rightarrow 2MO_{n/2} + nRCl$$

and the second route involves the reaction of a metal halide with an ether:

$$MCl_n + (n/2)ROR \rightarrow MO_{n/2} + nRCl$$

In both reactions, some of the driving force comes from the removal of the volatile product RCl. This first of the two methods has been employed by Colvin and co-workers [63] to prepare capped TiO$_2$ nanoparticles in refluxing heptadecane with trioctyl phosphine oxide as the capping agent:

$$MCl_n + M(OR)_n \rightarrow 2MO_{n/2} + nRCl$$
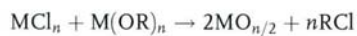
The particles formed clear solutions in non-polar solvents, from which they could be precipitated through the addition of a polar solvent such as acetone. When tri-octyl phosphine oxide was not taken with the starting materials, insoluble precipitates were obtained.

5.3.5
Solvothermal Methods

To prepare crystalline oxide materials, high temperatures, associated with the refluxing of reactants in high-boiling solvents, is often called for. There are many problems associated with such solvents, including possible toxicity, expense and their inability to dissolve simple salts. A simple method to circumvent this problem is to use solvothermal methods, employing solvents well above their boiling points in enclosed vessels that support high autogenous pressures. Solvothermal (called hydrothermal when the solvent is water) methods are widespread in their use, particularly in the preparation of crystalline solids, including silicate materials such as zeolites [64].

Recently, Rajamathi and Seshadri [65] have reviewed the uses of solvothermal methods for the preparation of oxide and chalcogenide nanoparticles. For oxide nanoparticles, these methods can involve hydrolysis, oxidation and thermolysis, all performed under hydrothermal or solvothermal conditions. Some of the more striking examples are provided here.

5.3.5.1 Oxidation

An unusual reaction reported by Inoue et al. [66] is the direct oxidation of Ce metal in 2-methoxyethanol at temperatures between 200 °C and 250 °C. Most of the product obtained was bulk CeO_2 as a yellow solid, but in addition, they obtained a brown solution of 2 nm CeO_2 nanoparticles. The CeO_2 nanoparticles could be salted out by the addition of NaCl, and redispersed into solution at will. The solutions obeyed the Beer–Lambert law for the concentration dependence of the optical extinction, suggesting that the nanoparticulate dispersion was a genuine solution.
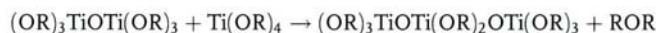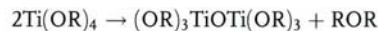
Starting with Zn powder and $GaCl_3$ in water, Qian and coworkers [67] have used the fact that the oxidation of Zn to Zn^{2+} in water is associated with the production of hydroxy ions according to:

$$Zn + 2H_2O \rightarrow Zn^{2+} + 2OH^- + H_2\uparrow$$
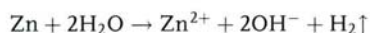
The OH^- ions help in the hydrolysis of Ga^{3+}, to eventually give, in the presence of Zn^{2+}, the spinel $ZnGa_2O_4$. The authors used a 10–20% over-stoichiometry of Zn and the reaction was carried out at 150 °C for 10 h. 10 nm $ZnGa_2O_4$ nanoparticles were obtained. Excess $ZnCl_2$ formed in the reaction could be washed away with water.

5.3.5.2 Hydrolysis

Chemseddine and Moritz [68] have used the polycondensation of titanium alkoxide $Ti(OR)_4$ in the presence of tetramethylammonium hydroxide, to obtain highly crystalline anatase nanoparticles with different sizes and shapes [Figure 5.4]. A general, stepwise reaction for such polycondensation could be written:

$$2Ti(OR)_4 \rightarrow (OR)_3TiOTi(OR)_3 + ROR$$

$$(OR)_3TiOTi(OR)_3 + Ti(OR)_4 \rightarrow (OR)_3TiOTi(OR)_2OTi(OR)_3 + ROR$$

and so on to anatase, though it might not proceed in precisely this manner in the presence of base. The reactions were performed in two steps: First, alkoxide was added to the base at 0 °C in alcoholic solvents in a three-necked flask. The temperature was then raised to reflux. The second stage involved treating the product of the reflux in Ti autoclaves under a saturated vapor pressure of water (2500 kPa) at temperatures between 175 °C and 200 °C for 5 h. The nanocrystals obtained were sufficiently monodisperse that they formed coherent superlattices, as monitored by low-angle powder X-ray diffraction. By using other hydroxides with bulkier alkyl groups (for example, tetrapropylammonium hydroxide) some control over crystallite morphology became possible.

Wu et al. [69] have combined microemulsion and inverse-micelle techniques with hydrothermal techniques in the preparation of rutile and anatase TiO_2 nanoparticles. They used the system water–cyclohexane–Triton X-100 with n-hexanol as a second emulsifier. The water-filled micellar pockets were acidified (with HCl or HNO_3) $Ti(OR)_4$ (R = butyl). Treating the system at 120–200 °C for 12–144 h gave anatase particles. When high HCl concentrations were employed, rutile rods were obtained.

Hirano [70] has prepared spinel $ZnGa_2O_4$ nanoparticles by adjusting the pH of Zn and Ga sulfates with NH_3 to different initial values (varied from 2.5 through 10). The material was heat-treated hydrothermally at temperatures between 150 °C and 240 °C for times between 5 and 50 h. Particle sizes could be varied from 5 to 25 nm.

Cabañas et al. [71] have described the preparation of nanoparticulate CeO_2–ZrO_2 solid solutions under *flow-hydrothermal* conditions, wherein the reactants are taken to the final temperature very rapidly in a continuous process. The advantage of performing hydrothermal reactions in such a manner is, firstly, that a large amount of material can be processed, permitting simple scale up. Secondly, the nucleation step can be made very rapid, as a result of the rapid heating. This can help separate nucleation and growth, and can thereby satisfy the famous LaMer criterion [72] for obtaining monodisperse particles. Cabañas and Poliakoff [73] have also prepared a number of spinel ferrite samples in this way, starting from mixtures of different Fe(II) and M(II) acetates (M = Co, Ni, Zn and Co/Ni). Most of the preparations yielded a bimodal distribution of sample sizes, with the smaller samples being about 10 nm in diameter and the larger ones, about 100 nm.

5.3.5.3 Thermolysis

Recently, Thimmaiah et al. [74] have extended the thermolytic route to oxide nanoparticles devised by Rockenberger, Scher and Alivisatos [57] to solvothermal conditions. Using solvothermal toluene (typically at 220 °C for 1 h), cupferron precursors of Fe, and Co and Fe are decomposed to obtain sub-12 nm maghemite γ-Fe_2O_3 nanoparticles and spinel $CoFe_2O_4$ nanoparticles. The reactions do not
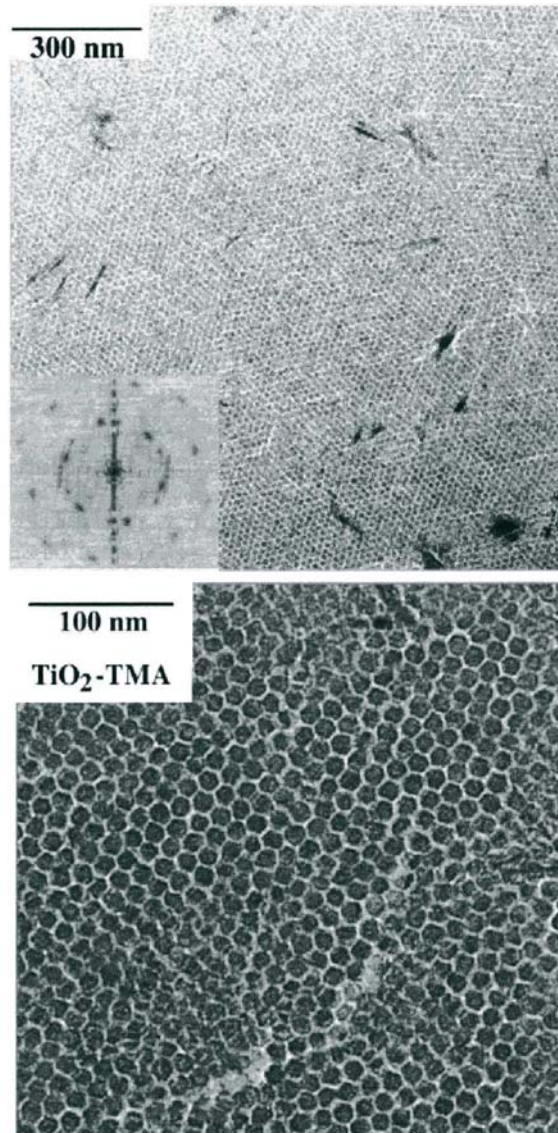
Fig. 5.4. Transmission electron micrographs of anatase TiO$_2$ nanoparticles prepared by solvothermal treatment of Ti(OR)$_4$ after hydrolysis with tetramethylammonium hydroxide. The inset in the upper micrograph displays a Fourier transform with discrete spots, attesting to the extent of superlattice coherence. The lower, high magnification image shows that the nanocrystals are well-faceted. Reproduced from [68] with permission from Wiley–VCH.
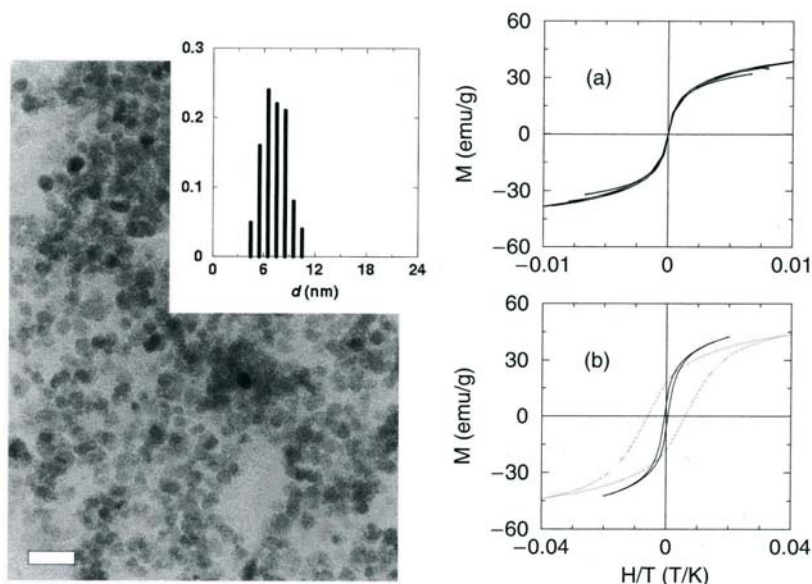
Fig. 5.5. Transmission electron micrograph of n-octylamine-capped spinel $CoFe_2O_4$ nanoparticles prepared by the thermolysis of Co(II) and Fe(III) cupferron precursors in solvothermal toluene. The panels on the right display the magnetic properties of these superparamagnetic particles. (a) is the M versus H/T plot for data on a pressed pellet of these nanoparticles taken at temperature of 300, 250, 200, 150 and 100 K, The collapse of all these traces onto a single S-shaped curve indicates superparamagnetic behavior. Only at 50 K and 5 K (black and gray traces in (b)) are the samples "blocked" and hysteretic behavior manifests. Reproduced from [74] with permission from the Royal Society of Chemistry.

work in the absence of long chain amines (n-octylamine and n-dodecylamine) which are added as capping agents. A complete characterization of the magnetic properties of these nanoparticles has been presented by the authors [Figure 5.5]. This is the only report to date of capped oxide nanoparticles prepared by a solvothermal route.

5.4
Prospects

As has been emphasized, research on the preparation of oxide nanoparticles is very much an active area that is being pursued across the world. While certain oxide structural classes (such as transition metal spinels) seem easily amenable to being prepared in nanoparticulate form, a number of other oxide materials are not. In particular, few attempts have been made to prepare capped perovskite oxide nanoparticles [61]. While some of the properties of oxide nanoparticles have already

been mentioned alongside their syntheses, some unusual properties and applications call for special mention.

Individual magnetic nanoparticles, apart from displaying superparamagnetic behavior, possess other unusual qualities. Bonet et al. [75] have shown that small ferrite (in the magnetoplumbite structure) nanoparticles can have their magnetic polarizations completely reversed through uniform rotation of their magnetization. The spin precession of the whole particle magnetic moment of 4 nm γ-Fe_2O_3 nanoparticles has been monitored, using neutron scattering, by Lefmann et al. [76]. These authors find that the precession is coherent since it is associated with the excitation of ferrimagnetism in the nanoparticle.

Oxide nanoparticles, unlike nanoparticles of metals, display an expansion in their lattice parameters in comparison with the bulk. Tsunekawa et al. have examined sub-10 nm CeO_{2-x} and sub-100 nm $BaTiO_3$ nanoparticles using a combination of electron diffraction, X-ray photoelectron spectroscopy and ab initio computer simulations. They find that in the CeO_{2-x} system, the lattice expansion arises from a decrease in Ce valence, whilst in the $BaTiO_3$ system, the decreasing Ti–O covalency with decreasing particle size results in the expanded lattice.

There is continued interest in magnetic oxide nanoparticle assemblies for magnetic data storage. Recent advances in this area have come from the group of Sun, who have prepared magnetite nanoparticles [77] from Fe(II) acetylacetonate in refluxing diphenyl ether in the presence of oleic acid and oleylamine. Precipitation by addition of ethanol gave 4 nm Fe_3O_4 nanoparticles which could be used to seed the growth of larger Fe_3O_4 particles (reaching 16 nm). The larger Fe_3O_4 nanoparticles can be oxidized to γ-Fe_2O_3 with a distinct powder XRD pattern. The same group [78] have then self-assembled these nanoparticles as well as performed coupled self-assemblies of Fe_3O_4 nanoparticles with Fe–Pt nanoparticles and then annealed the films to obtain exchange-coupled nanocomposite assemblies.

An interesting and novel application for magnetic nanoparticles is their use as intracellular magnetic labels in nuclear magnetic esonance imaging. The presence of magnetic nanoparticles results in protons in their vicinity relaxing at a much faster rate. Since NMR imaging is based on the rate of magnetic relaxation, there is distinct contrast introduced. Biocompatible dextran-coated nanoparticles have been conjugated with peptides to improve their uptake into target cells. These have then been found to significantly aid the NMR imaging of the cells [79]. Weissleder et al. have also conjugated specific oligonucleotide sequences to magnetic oxide nanoparticles [80]. This results in their being able to employ NMR methods in the rapid detection of DNA sequences that are complementary to the oligonucleotide that is bound to the nanoparticle. In functional magnetic resonance imaging (fMRI) experiments, primates or humans are exposed to some external stimulus while their brains are imaged. This technique has proved invaluable in mapping the brain, in terms of associating region with function. Magnetic nanoparticles (dextran-coated magnetite) have been used to enhance fMRI imaging contrast in the Rhesus brain in experiments that measured photic response [81].

Magnetic oxide nanoparticles are also finding a number of other uses, including in magnetic drug delivery and in hyperthermic cancer therapy. In the former, the

pharmacoactive molecule is bound to a small magnetic particle, and the particle is guided to its in vivo target through the use of magnetic fields. In the latter, cancerous tumors are destroyed by injecting magnetic particles into them and then coupling the particles to a strong radio-frequency magnetic field, resulting in large amounts of heats being delivered locally to, and eventually destroying, the tumor.

While heterogeneous catalysis is a traditional area of chemistry and is not usually classified as an application of nanoparticles, a recent development in cleaner-burning fuels is worth mentioning here. Two major manufacturers of diesel automobiles in Europe, Peugeot–Citröen and Ford, inject sub-10 nm CeO_2 nanoparticles (called by the trade name EOLYS TM, manufactured by the French company Rhodia) into diesel fuel before it is burnt in the engine. This results in an in situ catalyst that not only improves fuel efficiency but also greatly reduces the emission of particulates. Were the particles not sub-10 nm, it would not be possible to make homogeneous dispersions in the diesel fuel. It is expected that more than a million diesel automobiles will incorporate such systems by the year 2005. Another area where large quantities of nanoparticulate oxide materials are expected to be consumed is in the preparation of transparent sunscreens for topical application. Traditionally, sunscreens are applied as opaque creams. The active principle is a ZnO powder that absorbs most of the UV radiation incident upon the skin. There is great interest however, in material that can be sprayed on, and that is invisible. For this, the ZnO particles have to be sub-100 nm.

Acknowledgments

References

1 M. FARADAY, *Philos. Trans. R. Soc. London*, **1857**, *147*, 145–181.

2 M. JOSÉ-YACAMÁN, L. RENDÓN, J. ARENAS et al., *Science*, **1996**, *273*, 223–225.

3 Oxford English Dictionary at http://dictionary.oed.com/

4 A. FOJTIK, H. WELLER, U. KOCH et al., *Ber. Bunsen-Ges. Phys. Chem.*, **1984**, *88*, 969–977.

5 M. L. STEIGERWALD, A. P. ALIVISATOS,

J. M. GIBSON et al., *J. Am. Chem. Soc.*, **1988**, *110*, 3046–3050.

6 C. B. MURRAY, D. J. NORRIS, M. G. BAWENDI, *J. Am. Chem. Soc.*, **1993**, *115*, 8706–8715.

7 M. BRUST, M. WALKER, D. BETHELL et al., *J. Chem. Soc., Chem. Commun.*, **1994**, 801–802.

8 R. G. NUZZO, D. L. ALLARA, *J. Am. Chem. Soc.*, **1983**, *105*, 4481–4483.

9 J. Prost, F. Rondelez, Suppl. to *Nature*, **1991**, *350*, 11–23.

10 A. Chemseddine, H. Weller, *Ber. Bunsen-Ges. Phys. Chem.*, **1993**, *97*, 636–637.

11 M. D. Bentzon, J. van Wonterghem, S. Mørup et al., *Philos. Mag. B*, **1989**, *60*, 169–178.

12 C. B. Murray, C. R. Kagan, M. G. Bawendi, *Science*, **1995**, *270*, 1335–1338.

13 R. L. Whetten, J. T. Khoury, M. M. Alvarez et al., *Adv. Mater.*, **1996**, *8*, 428–433.

14 C. P. Collier, T. Vossmeyer, J. R. Heath, *Annu. Rev. Phys. Chem.*, **1998**, *49*, 371–404; R. L. Whetten, M. N. Shafigullin, J. T. Khoury et al., *Acc. Chem. Res.*, **1999**, *32*, 397–406; C. B. Murray, C. R. Kagan, M. G. Bawendi, *Annu. Rev. Mater. Sci.*, **2000**, *30*, 545–610.

15 J. V. Sanders, *Acta Crystallogr. Sect. A*, **1968**, *24*, 427–434.

16 See for example, R. J. Cava, *J. Am. Ceram. Soc.*, **2000**, *83*, 5–28.

17 See for example, J. Z. Sun and A. Gupta, *Annu. Rev. Mater. Sci.*, **1998**, *28*, 45–78.

18 A. I. Kingon, J.-P. Maria, S. K. Streiffer, *Nature*, **2000**, *406*, 1032–1038.

19 J. F. Scott, *Annu. Rev. Mater. Sci.*, **1998**, *28*, 79–100.

20 O. Auciello, J. F. Scott, R. Ramesh, *Physics Today*, July **1998**, 22–27.

21 D. Dimos, C. H. Mueller, *Annu. Rev. Mater. Sci.*, **1998**, *28*, 397–419.

22 B. C. H. Steele, A. K. Heinzel, *Nature*, **2001**, *414*, 345–352.

23 J.-M. Tarascon, M. Armand, *Nature*, **2001**, *414*, 359–367.

24 H. Gleiter, *Acta Mater.*, **2000**, *48*, 1–29.

25 R. Blakemore, *Science*, **1975**, *190*, 377–379.

26 R. B. Frankel, R. P. Blakemore, R. S. Wolfe, *Science*, **1979**, *203*, 1355–1356.

27 J. L. Kirschvink, M. M. Walker, C. E. Diebel, *Curr. Opin. Neurobiol.*, **2001**, *11*, 462–467.

28 M. M. Walker, T. E. Dennis, J. L. Kirschvink, *Curr. Opin. Neurobiol.*, **2002**, *12*, 735–744.

29 R. E. Dunin-Borkowski, M. R. McCartney, R. B. Frankel et al., *Science*, **1998**, *282*, 1868.

30 D. Schüller, R. B. Frankel, *Appl. Microbial Biotechnol.*, **1999**, *52*, 464–473.

31 http://www.nanomagnetics.co.uk

32 K. L. Thomas-Keprta, D. A. Bazylinski, J. L. Kirschvink et al., *Geochim. Cosmochim. Acta*, **2000**, *64*, 4049–4081.

33 P. R. Buseck, R. E. Dunin-Borkowski, B. Devouard et al., *Proc. Natl. Acad. Sci. U.S.A.*, **2001**, *98*, 13490–13495.

34 D. F. Shriver, P. W. Atkins, *Inorganic Chemistry*, 3rd edition., W. H. Freeman and Company, New York.

35 G. H. A. Therese, P. Vishnu Kamath, *Chem. Mater.*, **2000**, *12*, 1195–1204.

36 V. Cabuil, *Curr. Opin. Colloid Interface Sci.*, **2000**, *5*, 44–48.

37 J. P. Chen, C. M. Sorenson, K. J. Klabunde et al., *Phys. Rev. B*, **1996**, *54*, 9288–9296.

38 S. Lefebure, E. Dubois, V. Cabuil et al., *J. Mater. Res.*, **1998**, 2975–2981.

39 R. Massart, E. Dubois, V. Cabuil et al., *J. Magn. Magn. Mater.*, **1995**, *149*, 1–5.

40 M. P. Morales, S. Veintemillas-Verdaguer, M. I. Montero et al., *Chem. Mater.*, **1999**, *11*, 3035–3064.

41 S. Ammar, A. Helfen, N. Jouini et al., *J. Mater. Chem.*, **2001**, *11*, 186–192.

42 M. Rajamathi, M. Ghosh, R. Seshadri, *J. Chem. Soc., Chem. Commun.*, **2002**, 1152–1153.

43 D. Carunto, Y. Remond, N. H. Chou et al., *Inorg. Chem.*, **2002**, *41*, 6137–6146.

44 M. P. Pileni, *J. Phys. Chem.*, **1993**, *97*, 6961–6973; *Langmuir*, **1997**, *13*, 3266–3276.

45 V. Pillai, D. O. Shah, *J. Magn. Magn. Mater.*, **1996**, *163*, 243–248.

46 C. Liu, Z. J. Zhang, *Chem. Mater.*, **2001**, *13*, 2092–2096.

47 C. Vestal, Z. J. Zhang, *Chem. Mater.*, **2002**, *14*, 3817–3822.

48 M. Moumen, M. P. Pileni, *Chem. Mater.*, **1996**, *8*, 1128–1134; *J. Phys. Chem.*, **1996**, *100*, 1867–1873; M.

MOUMEN, P. BONNEVILLE, M. P. PILENI, *J. Phys. Chem.*, **1996**, *100*, 14410–14416.

49 J. F. HOCHEPIED, Ph. SAINCTAVIT, M. P. PILENI, *J. Magn. Magn. Mater.*, **2001**, *231*, 315–322.

50 J. F. HOCHEPIED, P. BONNEVILLE, M. P. PILENI, *J. Phys. Chem.*, **2000**, *104*, 905–912.

51 A. T. NGO, M. P. PILENI, *J. Phys. Chem.*, **2001**, *105*, 53–58.

52 R. VIJAYA KUMAR, Y. DIAMANT, A. GEDANKEN, *Chem. Mater.*, **2000**, *12*, 2301–2305.

53 R. VIJAYA KUMAR, Y. KOLTYPIN, X. N. XU et al., *J. Appl. Phys.*, **2001**, *89*, 6324–6328.

54 T. HYEON, S. S. LEE, J. PARK et al., *J. Am. Chem. Soc.*, **2001**, *123*, 12798–12801.

55 J. A. NELSON, M. J. WAGNER, *Chem. Mater.*, **2002**, *14*, 915–917.

56 J. A. NELSON, E. L. BRANT, M. J. WAGNER, *Chem. Mater.*, **2003**, *15*, 688–693.

57 J. ROCKENBERGER, R. C. SCHER, A. P. ALIVISATOS, *J. Am. Chem. Soc.*, **1999**, *121*, 11595–11596.

58 A. K. BOAL, K. DAS, M. GRAY, V. M. ROTELLO, *Chem. Mater.*, **2002**, *14*, 2628–2636.

59 A. B. BOURLINOS, A. SIMOPOULOS, D. PETRIDES, *Chem. Mater.*, **2002**, *14*, 899–903.

60 A. B. BOURLINOS, A. BAKANDRITSOS, V. GEORGAKILAS et al., *Chem. Mater.*, **2002**, *14*, 3226–3228.

61 S. O'BRIEN, L. BRUS, C. B. MURRAY, *J. Am. Chem. Soc.*, **2001**, *123*, 12085–12086.

62 P. ARNAL, R. J. P. CORRIU, D. LECLERCQ et al., *Chem. Mater.*, **1997**, *9*, 694–698.

63 T. J. TRENTLER, T. E. DENLER, J. F. BERTONE et al., *J. Am. Chem. Soc.*, **1999**, *121*, 1613–1614.

64 K. BYRAPPA, M. YOSHIMURA, *Handbook of Hydrothermal Technology*, William Andrew Publishing, Norwich, New York 2001.

65 M. RAJAMATHI, R. SESHADRI, *Curr. Opin. Solid State Mater. Sci.*, **2002**, *6*, 337–345.

66 M. INOUE, M. KIMURA, T. INUI, *J. Chem. Soc., Chem. Commun.*, **1999**, 957–958.

67 Y. LI, X. DUAN, H. LIAO, Y. QIAN, *Chem. Mater.*, **1998**, *10*, 17–18.

68 A. CHEMSEDDINE, T. MORITZ, *Eur. J. Inorg. Chem.*, **1999**, 235–245.

69 M. WU, J. LONG, A. HUANG, Y. LUO et al., *Langmuir*, **1999**, *15*, 8822–8825.

70 M. HIRANO, *J. Mater. Chem.*, **2000**, *10*, 469–472.

71 A. CABAÑAS, J. A. DARR, E. LESTER et al., *J. Chem. Soc., Chem. Commun.*, **2000**, 901–902; *J. Mater. Chem.*, **2001**, *11*, 561–568.

72 V. K. LAMER, R. H. DINEGAR, *J. Am. Chem. Soc.*, **1950**, *72*, 4847.

73 A. CABAÑAS, M. POLIAKOFF, *J. Mater. Chem.*, **2001**, *11*, 1408–1416.

74 S. THIMMAIAH, M. RAJAMATHI, N. SINGH et al., *J. Mater. Chem.*, **2001**, *11*, 3215–3220.

75 E. BONET, W. WERNSDORFER, B. BARBARA et al., *Phys. Rev. Lett.*, **1999**, *83*, 4188–4191.

76 K. LEFMANN, F. BØDKER, S. N. KLAUSEN et al., *Europhys. Lett.*, **2001**, *54*, 526–532.

77 S. SUN, H. ZENG, *J. Am. Chem. Soc.*, **2002**, *124*, 8204–8205.

78 H. ZENG, J. LI, Z. L. WANG et al., *Nature*, **2002**, *420*, 395–398.

79 L. JOSEPHSON, C.-H. TUNG, A. MOORE et al., *Bioconjugate Chem.*, **1999**, *10*, 186–191.

80 L. JOSEPHSON, J. M. PEREZ, R. WEISSLEDER, *Angew. Chem. Intl. Ed. Engl.*, **2001**, *40*, 3204–3206.

81 D. J. DUBOWITZ, K. A. BERNHEIM, D.-Y. CHEN et al., *NeuroReport*, **2001**, *12*, 2335–2340.